Resolving multiple peaks using a sub-transit-linewidth cross-correlation resonance

Pengxiong Li, Lei Feng, and Yanhong Xiao*

Department of Physics, State Key Laboratory of Surface Physics, Key Laboratory of Micro and Nano Photonic Structures (Ministry of Education), Fudan University, Shanghai 200433, China

(Received 21 January 2014; published 22 April 2014)

In a recent paper [L. Feng *et al.*, Phys. Rev. Lett. **109**, 233006 (2012)], we demonstrated a sub-transit-linewidth resonance based on cross correlation between optical fields in an electromagnetically induced transparency (EIT) system. Here, we investigate the ability of such resonance to resolve multiple resonance peaks. We first report the implementation of the cross-correlation resonance in a hyperfine EIT system, with a linewidth of about 1/16 of the transit EIT width. Then, a magnetic field is applied to create multipeak EIT resonance with tunable spacing. Cross-correlation resonance with multipeaks is observed and the line shape agrees qualitatively with our numerical simulations. We find that the multipeak correlation resonance has better contrast than the corresponding EIT resonance, but with a lower signal to noise. Furthermore, this correlation resonance cannot resolve peaks with spacing close to or less than the intrinsic width, like any other resonance techniques. We analyze the origin of this limitation and make connections to the Ramsey-type subnatural spectroscopy technique. This work shows potential applications of the correlation resonance in atomic frequency standard and laser spectroscopy.

DOI: 10.1103/PhysRevA.89.043835 PACS number(s): 42.50.Gy, 32.70.Jz, 42.62.Fi

I. INTRODUCTION

Narrow resonance techniques are useful for a wide variety of applications such as laser spectroscopy, precision measurements, frequency standards, sensing and imaging, etc. Resonance linewidth is usually limited by the lifetimes of the involved atomic states or the atom-light interaction time, which is named "intrinsic linewidth." However, there are several techniques that can overcome this limit, for instance, the Ramsey-type prepare-wait-probe technique [1–7], coupling a broad resonance to a narrower one [8–10], density narrowing [11], and the most recent cross-correlation resonance method [12]. In the latter approach, a linewidth that is 30 times below the intrinsic value was obtained experimentally, which as far as we know bears the highest narrowing factor in all the sub-intrinsic-linewidth experiments. For spectroscopy applications, the ability to resolve closely spaced multiple peaks is of interest. Therefore, for these sub-intrinsic-linewidth techniques, it is natural to investigate their ability to separate resonance lines spaced closer than the intrinsic linewidth, i.e., the possibility to break the "Rayleigh limit" in spectroscopy. It is the purpose of this paper to study the performance of the cross-correlation resonance in a multipeak resonance system.

The cross-correlation resonance uses the zero-time-lag cross correlation $g^{(2)}(0)$ between the intensity fluctuations in the two fields forming electromagnetically induced transparency (EIT) as the observable, where the intensity noise is converted from the laser's phase noise (PN-IN) by atom-light interactions. The Scully group [13,14] as well as the Nussenzveig group and their collaborators [15–17] were among the first ones to study this resonance, using the random-phase noise in a diode laser. It was found that the resonance linewidth was narrower than that of the EIT [18], but it was unclear what determines the resonance linewidth and what the limit was. By introducing artificial noise, i.e, frequency modulation in the laser, and by comparing $g^{(2)}(0)$ resonance using diode lasers with different linewidths, we found that the $g^{(2)}(0)$ resonance linewidth can be much smaller than the intrinsic width [12,19], which depends on the magnitude of the laser noise, and is limited only by noises in the system. All of the previous experiments on $g^{(2)}(0)$ resonance used Zeeman sublevels as EIT ground states, and the single $g^{(2)}(0)$ resonance was studied. Here, in order to study the multipeak resonance, we used a hyperfine nondegenerate EIT system, where a magnetic field was applied to create spacing between three EIT peaks. We first confirmed that with $B = 0$, the single $g^{(2)}(0)$ resonance in the hyperfine system can have sub-intrinsic linewidth. Then we measured the multipeak $g^{(2)}(0)$ resonance spectrum for various peak spacings. The observed line shapes agree well with our numerical calculations. We found that the multipeak correlation resonance has better contrast than the multipeak EIT, but the ultimate "Rayleigh limit" could not be surpassed. We describe the physics behind this result and relate our observations to a similar multipeak resolving behavior of a Ramsey-type method [7].

Before proceeding, we review the key characteristics of the $g^{(2)}(0)$ correlation resonance in a single Λ system. The full line shape of a single resonance $g^{(2)}(0)$ spectrum has four regions, as described in [18,19]. The first region is the central peak, featuring a sharp transition from correlation to anticorrelation, whose linewidth is smaller than the intrinsic width. Anticorrelation in this region is caused by the nonzero imaginary part in the ground-state coherence [16], which induces the Raman-type photon fluctuations in the two EIT fields, i.e, one field absorbs a photon and the other emits, forming anticorrelation photon statistics. An alternative picture is that the strong nonlinearity associated with the ground-state coherence induces a large offset (much greater than two-photon detuning) between the transmission spectra of the two EIT fields and creates opposite PN-IN conversion slopes, causing anticorrelation. As two-photon detuning increases, anticorrelation changes towards correlation (the second region), forming the wing structure whose linewidth is on the same scale of the EIT width and increases with the laser power. For even larger two-photon detunings, $g^{(2)}(0)$ turns

*Corresponding author: yxiao@fudan.edu.cn

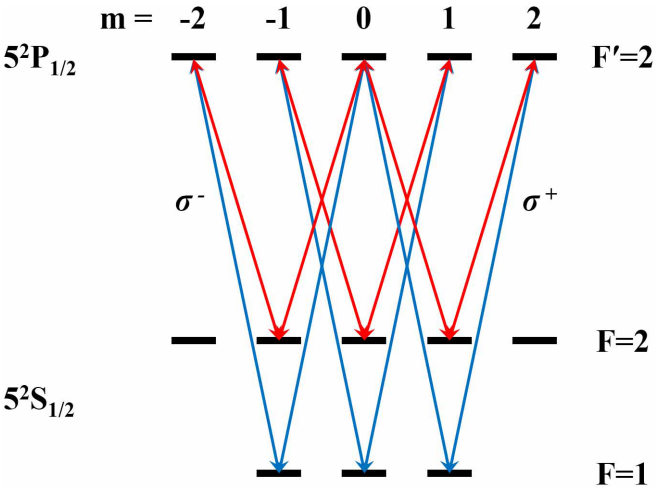

FIG. 1. (Color online) Energy levels for the multipeak hyperfine EIT using two orthogonal linearly polarized laser fields.

towards negative again (the third region). In this region, the ground-state coherence is negligible and anticorrelation forms because the two transmission spectra are offset by an amount equal to two-photon detuning, giving rise to opposite PN-IN slopes again. Lastly, when two-photon detuning is much larger than the one-photon resonance linewidth (the fourth region), correlation reappears.

II. EXPERIMENT

Our experiment employed hyperfine EIT (Fig. 1) in a ^{87}Rb vacuum vapor cell, formed by transitions from $5S_{1/2}, F = 2,1$ to $5P_{1/2}, F' = 2$. As shown in Fig. 2, an external cavity diode laser with a small linewidth (less than 1 MHz) was frequency modulated through the piezo transducer (PZT) voltage, and its power was then boosted by a tapered amplifier. The amplifier output was split into two beams. One goes through an electro-optic modulator (EOM) to produce small sidebands at 6.8 GHz, and then through a Fabry-Perot (FP) cavity to let through only the first-order upper sideband. This beam then recombines with the other bypass channel via a polarization beam splitter. A half-wave plate was added in the bypass channel for adjustment of its power, and together with other wave plates to vary the power ratio of the two CPT fields and the total power as well. To mitigate conversion of laser frequency modulation to intensity modulation by the FP cavity, we slightly misalign the cavity to broaden the cavity resonance. With about the same laser power, the combined beams then entered a polarization maintaining single-mode fiber mainly for ideal spatial overlap. It has been demonstrated that hyperfine EIT with orthogonal linearly polarized fields has high contrast [20], and here this configuration also allows easy separation of the two EIT fields at the cell output through polarization. The $g^{(2)}(0)$ value was computed using the ac signals in the two EIT fields. The solenoid within the magnetic shield produces a homogeneous magnetic field along the light propagation direction, which produces three sets of EIT resonances (Fig. 1) with spacing tunable via the strength of the magnetic field. The vapor cell was maintained at 53 °C by resistive heating along the outer surface of the innermost shield.

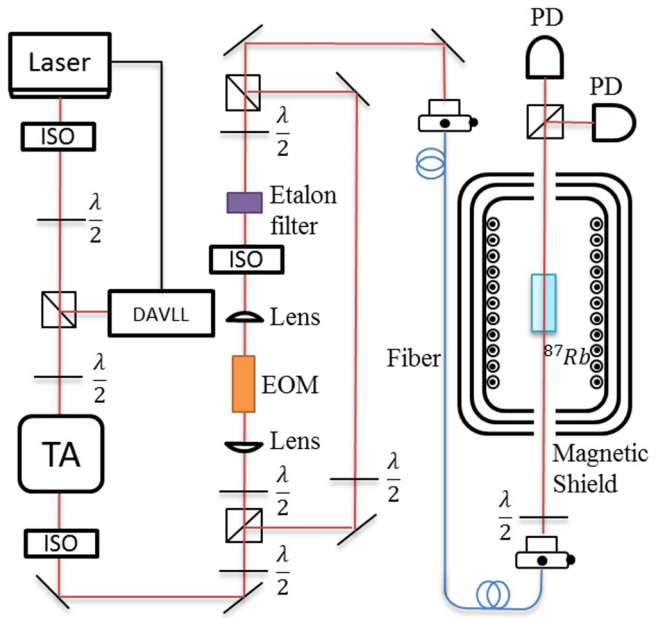

FIG. 2. (Color online) The experiment schematics. See text for details.

First, we measured the single-peak $g^{(2)}(0)$ spectra when the magnetic field was turned off. The laser frequency was modulated at 10.3 kHz with a modulation range of about 11 MHz. The total laser power at the cell input was 26 μW, with the beam diameter of 1 mm. The center frequency of the laser was locked using a dichroic atomic vapor laser lock (DAVLL) system [21]. The two-photon detuning Δ was adjusted through the modulation frequency of the EOM. The $g^{(2)}(0)$ value was computed for each Δ, yielding a $g^{(2)}(0)$ resonance spectrum as shown in Fig. 3. The FWHM was 11.7 kHz, which is about 1/16 of the zero-power EIT linewidth 190 kHz extracted from our measured EIT width vs laser power curve (not shown).

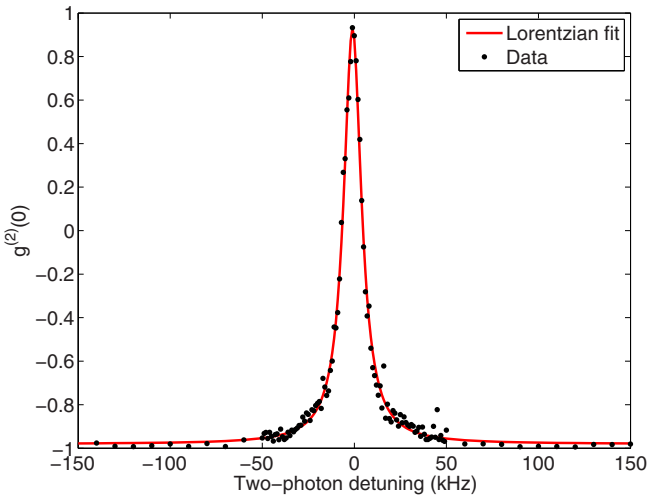

FIG. 3. (Color online) Measured single-peak $g^{(2)}(0)$ resonance spectrum. The FWHM is about 11.6 kHz, which is 1/16 of the transit EIT width of 190 kHz. The total laser power at the cell input is 26 μW.

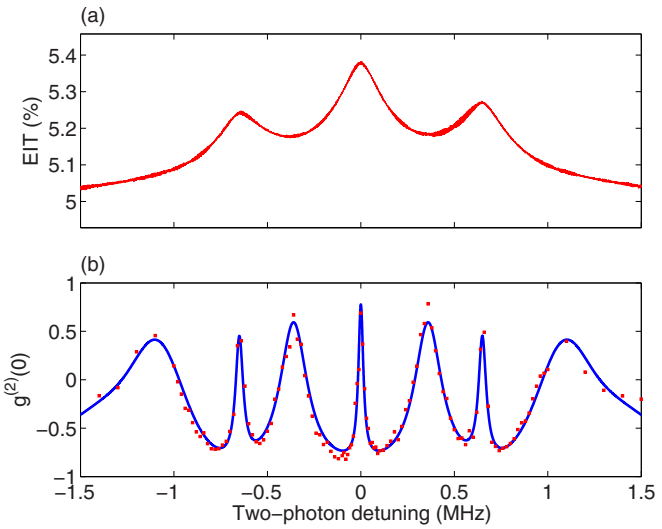

FIG. 4. (Color online) Measured EIT and $g^{(2)}(0)$ spectra for peak spacing equal to 3.5 times the transit EIT FWHM. (a) EIT spectrum. (b) $g^{(2)}(0)$ spectrum. The blue curve is to guide the eye. Total laser power was 26 μW for both (a) and (b).

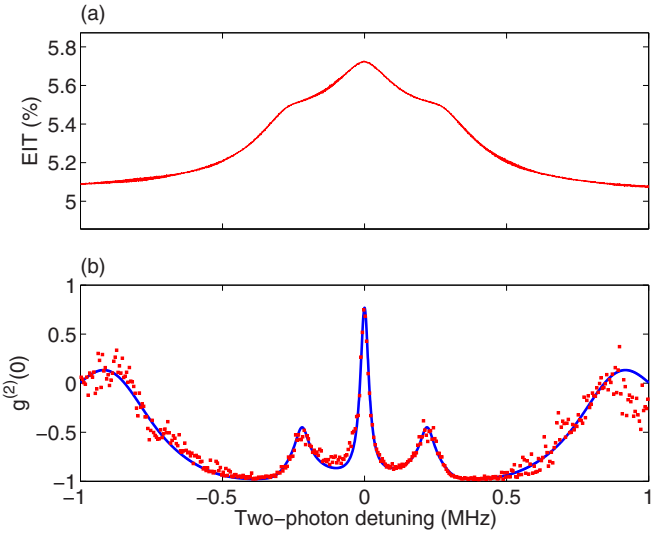

FIG. 5. (Color online) Measured EIT and $g^{(2)}(0)$ spectra for peak spacing equal to 1.5 times the transit EIT FWHM. (a) EIT spectrum. (b) $g^{(2)}(0)$ spectrum. The blue curve is to guide the eye. Total laser power was 26 μW for both (a) and (b).

This zero-power EIT linewidth is close to the calculated transit linewidth from the measured laser beam size. Therefore, the intrinsic EIT linewidth in our system is set by the transit width.

Next, we turn to the case of multiple hyperfine EIT resonances. When a magnetic field is applied, the single EIT resonance is split into three peaks due to the opposite signs of the g factors for the $F = 2$ and $F = 1$ ground states. Every EIT peak is the constructive interference of two Λ systems, each formed by the circular polarization components of the same helicity in the two orthogonal linearly polarized optical fields [20]. The contrast of the multiple EIT peaks is lower than that of the single EIT resonance above, and thus we increased the frequency modulation range to 27.2 MHz for better $g^{(2)}(0)$ resonance contrast. The spacing d between neighboring EIT peaks was adjusted through the magnetic field. Figure 4 shows the EIT resonance and the $g^{(2)}(0)$ resonance for a spacing equal to 3.5 times the zero-power EIT FWHM. The three EIT peaks are partially overlapped due to moderate power broadening, while the corresponding $g^{(2)}(0)$ peaks are well separated because of the sub-transit linewidth. The additional "artifact" peaks between the "real" narrow $g^{(2)}(0)$ peaks are from the influence of the power-broadened wing structure in the $g^{(2)}(0)$ spectra [18,19], as mentioned above. When the peak spacing is 1.5 times the zero-power EIT FWHM (Fig. 5), the three EIT peaks show poor contrast, but the $g^{(2)}(0)$ spectra still have pronounced peaks. There are only three peaks now because the artifact peaks have merged with the "real" peaks. When the spacing approaches the zero-power EIT FWHM, i.e., at the "spectroscopy Rayleigh limit," both EIT and $g^{(2)}(0)$ spectra fail to resolve the three peaks.

III. NUMERICAL SIMULATION

The above observations are in good qualitative agreement with our simulations. To simplify calculations without missing the key physics, a much less complicated multilevel system as shown in Fig. 6 was considered. Laser field E_1 couples the ground state $|1\rangle$ to the excited state $|e\rangle$, and E_2 couples three equally spaced states $|2\rangle$,$|3\rangle$,$|4\rangle$ to $|e\rangle$. The coherence decay rate between $|1\rangle$ and 2–4 is γ_2, giving rise to an intrinsic EIT FWHM of $2\gamma_2$. Coherence within the three ground states 2–4 was neglected. The phase of the two fields undergoes the same phase modulation. Figure 7 shows the simulation results. When states 2–4 have a spacing equal to 3.5 times $2\gamma_2$, we can see clearly five peaks in the spectrum, with two being the artifact peaks. When the spacing was reduced to 1.5 times $2\gamma_2$, the artifact peak and the $g^{(2)}(0)$ side peaks merge together and only three peaks appear in the $g^{(2)}(0)$ spectra. The two side peaks in the EIT spectrum for the same laser

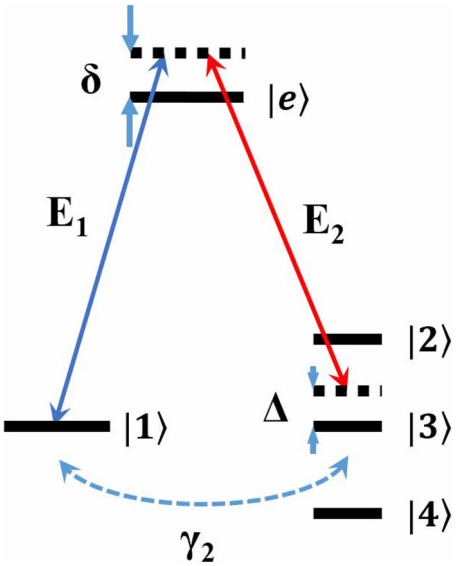

FIG. 6. (Color online) Simplified energy levels for the multipeak EIT used in our simulation.

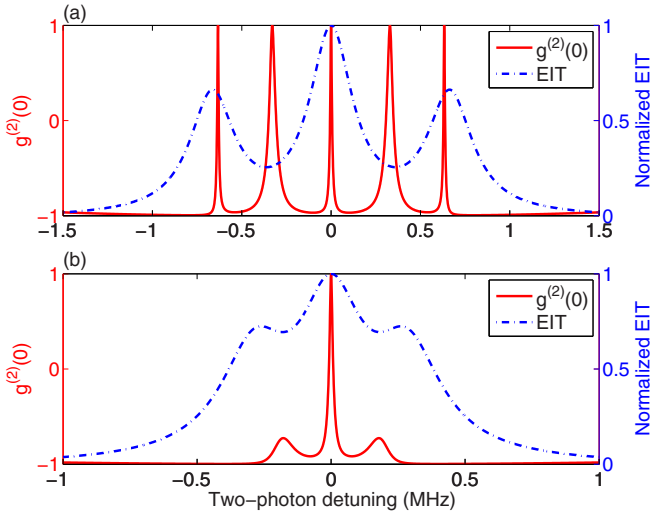

FIG. 7. (Color online) Simulation results of the three Λ energy system. In (a), the level spacing was 3.5 times the transit EIT FWHM. Both EIT and $g^{(2)}(0)$ resonance can resolve the energy levels. In (b), the level spacing was 1.5 times the transit EIT FWHM. The EIT peaks begin to overlap, and the $g^{(2)}(0)$ shows individual peaks well. See text for details.

power have a lower contrast than that in $g^{(2)}(0)$. We note that, compared to the numerical result, the experimental $g^{(2)}(0)$ spectra curved down at large one-photon detunings, which is due to the anticorrelation effect from the two independent one-photon resonance, as mentioned in the third paragraph above. Numerical calculation has this curve-down at much larger two-photon detuning. This discrepancy may come from the fact that we used an excited-state decay rate of 500 MHz to phenomenologically account for Doppler broadening.

IV. DISCUSSION

In general, as described in our previous work, the $g^{(2)}(0)$ spectrum has a narrower linewidth but a lower signal-to-noise ratio (SNR) compared to traditional spectroscopy methods where the dc absorption is often measured. The resolving power, i.e., the ratio of the resonance linewidth to SNR, is usually higher for the $g^{(2)}(0)$ method due to its better immunity to technical noises, since we have effectively used phase-sensitive detection because the ac transmission traces were triggered against the modulation signal. Here, the hyperfine $g^{(2)}(0)$ resonance shows a slight superiority in resolving power. The optimized single-peak hyperfine EIT resonance has a SNR of 900 in a detection time of 16 ms, and the resolving power is 430 Hz; the $g^{(2)}(0)$ spectrum has a SNR of 100, and the resolving power is 230 Hz. The resolving power was only enhanced by about two times, mainly because of additional noises that the $g^{(2)}(0)$ measurement is subject to. The dominant noise source was the intensity modulation converted by the filtering etalon from the laser frequency modulation, and this AM was measured to be about 0.4% of the dc transmission, comparable to the minimal phase-modulation to amplitude-modulation conversion (PM-AM) signal (occurring at zero two-photon detuning) wanted for the $g^{(2)}(0)$. This has broadened the $g^{(2)}(0)$ resonance. The residual amplitude modulation (RAM) in the laser was about 0.1%, but its phase was unstable, and therefore most of it could be averaged out. The EOM modulation depth was relatively low and the first-order sideband was about 10% of the carrier. The leaked carrier power from the etalon was about 4% of the transmitted first-order sideband, which slightly degrades the EIT contrast and also broadens the $g^{(2)}(0)$ resonance. In addition, there are some random noise sources such as intensity noise from the BoosTA tapered amplifier, electronics noise from the photodetectors, and, most importantly, the 6.8 GHz rf amplifier [22] has unusually large intensity noise in the kHz range, which brought low-frequency intensity noise in one of the EIT fields with a relative intensity noise (RIN) level of about 3%. Luckily, these random noises were removed to a large extent by the phase-sensitive detection.

In the case of multiple resonance peaks, the $g^{(2)}(0)$ resonance showed better contrast but worse SNR than the EIT resonance. Also, the two side $g^{(2)}(0)$ peaks are more shifted from the resonance position than the corresponding EIT side peaks, as seen in both our numerical calculation and experiment. This shift has to do with the wide wing structure of the $g^{(2)}(0)$ resonance, which has a power-broadened linewidth, as mentioned in the third paragraph. The $g^{(2)}(0)$ wing structure of the middle resonance "pushes away" the side $g^{(2)}(0)$ peaks. However, the middle $g^{(2)}(0)$ resonance peak remains unshifted because the influences from the two side $g^{(2)}(0)$ resonances cancel each other, which indicates that such shift does no harm to atomic-clock applications. On the other hand, this excess sensitivity of the peak location to nearby resonances might make $g^{(2)}(0)$ resonance useful for sensing.

It is worth noting that although the $g^{(2)}(0)$ resonance is a type of FM spectroscopy, it is distinct from conventional FM spectroscopy. Traditionally, frequency modulation is imposed on the frequency representing the x axis of a spectrum, and the phase-sensitive detection yields a zero crossing at the resonance center. However, in the $g^{(2)}(0)$ resonance, the frequency modulation is applied to the common one-photon detuning of the two EIT fields, and hence phase-sensitive detection of the total output intensity generally cannot produce a zero crossing at the EIT resonance. If the $g^{(2)}(0)$ resonance is used for atomic clocks, phase or frequency modulation of the two-photon detuning is needed to produce a zero crossing at the EIT resonance center, as exactly occurs in the CPT atomic clocks. The remaining question is how to incorporate the computation process of $g^{(2)}(0)$ in the clock operation. This can be done by a data processing chip integrated in the detection system and should not add much extra time. The time-consuming part is to take the time traces, whose length should be at least 10 times the modulation period of the laser for proper $g^{(2)}(0)$ extraction. Here we have averaged for 16 ms for each $g^{(2)}(0)$ value for better SNR, but this is because of technical noise in the experiment and such average is also needed in the traditional EIT measurement. Most importantly, since the $g^{(2)}(0)$ resonance technique can work at high modulation frequencies up to about 500 MHz (the Doppler width), the time trace can be made much shorter than the dwell time of the two-photon detuning sweep, which is at least the inverse of the optical pumping rate to avoid transits or distortion in EIT spectra. In brief, computing the $g^{(2)}(0)$ value is not an issue for its application in atomic clocks.

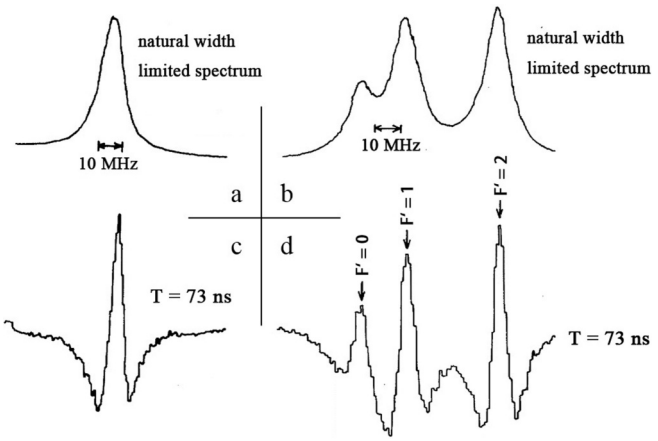

FIG. 8. Experiment results from the time-delayed subnatural Ramsey resonance. Traditional absorption spectra for a (a) single peak and (b) three-peak case. (c),(d) Corresponding Ramsey spectra of (a) and (b). Adapted from figures in [7].

Finally, we point out that our $g^{(2)}(0)$ resonance method has very similar performance to the Ramsey-type subnatural linewidth technique [1–7]. For instance, in Ref. [7], a Ramsey fringe with subnatural linewidth was obtained by choosing a dark evolution time longer than the natural lifetime. Figure 8 summarizes their main results. Figures 8(a) and 8(b) are traditional absorption spectrum for a single- and multipeak resonance, respectively, and Figs. 8(c) and 8(d) are their corresponding Ramsey spectra. As can be seen, the Ramsey spectra has a fringe linewidth that is about half of the natural linewidth, but its signal to noise is worse. In the multipeak case, the traditional method cannot completely separate the left two peaks, whose spacing is 1.5 times the natural linewidth, but the Ramsey spectrum can separate them better (i.e., higher contrast), again with a much worse signal to noise. Between the two "real" peaks on the right side, there is also an "artifact" peak. This has a similar origin to the "artifact" peak in our $g^{(2)}(0)$ case. As we know, other than the central fringe, a Ramsey spectrum has many fringes and an envelope as well. It is precisely these side structures that give rise to the artifact peak. For the left two peaks in Fig. 8(d), the artifact peak merges with the real peak when the spacing of two resonance peaks is close to the natural width, which is also similar to the case shown in Fig. 5.

V. CONCLUSION

In conclusion, we demonstrated the sub-transit-linewidth cross-correlation resonance in a hyperfine EIT system, and studied its behavior in the multipeak regime. It was found that, for the single resonance case, this correlation resonance has a higher resolving power than the EIT resonance; for the multipeak case, it has higher contrast but lower signal to noise than EIT. The observed multipeak resonance line shapes agree well with our simulations. We have identified the resemblance between our method and a Ramsey-type spectroscopy in their ability to resolve multipeaks. These results show that the correlation resonance has potential applications in atomic clocks, atomic magnetometry, and laser spectroscopy.

ACKNOWLEDGMENTS

We thank one of the anonymous referees of our previous paper [12] for stimulating this study through the referee report. This work was funded by the NBRPC (973 Program Grants No. 2012CB921604 and No. 2011CB921604), NNSFC (Grants No. 61078013 and No. 10904018), and the Research Fund for the Doctoral Program of Higher Education of China.

[1] M. A. Dugan and A. C. Albrecht, Phys. Rev. A **43**, 3877 (1991).
[2] M. A. Dugan and A. C. Albrecht, Phys. Rev. A **43**, 3922 (1991).
[3] J. Hald, J. C. Petersen, and J. Henningsen, Phys. Rev. Lett. **98**, 213902 (2007).
[4] P. L. Knight and P. E. Coleman, J. Phys. B **13**, 4345 (1980).
[5] H. W. Lee, P. Meystre, and M. O. Scully, Phys. Rev. A **24**, 1914 (1981).
[6] H. Metcalf and W. Phillips, Opt. Lett. **5**, 540 (1980).
[7] F. Shimizu, K. Umezu, and H. Takuma, Phys. Rev. Lett. **47**, 825 (1981).
[8] W. Gawlik, J. Kowalski, F. Trager, and M. Vollmer, Phys. Rev. Lett. **48**, 871 (1982).
[9] J. F. Lam, D. G. Steel, and R. A. McFarlane, Phys. Rev. Lett. **56**, 1679 (1986).
[10] D. J. Gauthier, Y. Zhu, and T. W. Mossberg, Phys. Rev. Lett. **66**, 2460 (1991).
[11] A. Godone, F. Levi, and S. Micalizio, Phys. Rev. A **65**, 031804 (2002).
[12] L. Feng, P. X. Li, L. Jiang, J. M. Wen, and Y. H. Xiao, Phys. Rev. Lett. **109**, 233006 (2012).
[13] V. A. Sautenkov, Y. V. Rostovtsev, and M. O. Scully, Phys. Rev. A **72**, 065801 (2005).
[14] G. O. Ariunbold, Y. V. Rostovtsev, V. A. Sautenkov, and M. O. Scully, J. Mod. Opt. **57**, 1417 (2010).
[15] L. S. Cruz, D. Felinto, J. Gomez, M. Martinelli, P. Valente, A. Lezama, and P. Nussenzveig, Eur. Phys. J. D **41**, 531 (2007).
[16] D. Felinto, L. S. Cruz, R. A. de Oliveira, H. M. Florez, M. H. G. de Miranda, P. Nussenzveig, M. Martinelli, and J. W. R. Tabosa, Opt. Express **21**, 1512 (2013).
[17] H. M. Florez, L. S. Cruz, M. H. G. de Miranda, R. A. de Oliveira, J. W. R. Tabosa, M. Martinelli, and D. Felinto, Phys. Rev. A **88**, 033812 (2013).
[18] Y. Xiao, T. Wang, M. Baryakhtar, M. Van Camp, M. Crescimanno, M. Hohensee, L. Jiang, D. F. Phillips, M. D. Lukin, S. F. Yelin *et al.*, Phys. Rev. A **80**, 041805 (2009).
[19] L. Feng, P. X. Li, M. Z. Zhang, T. Wang, and Y. H. Xiao, Phys. Rev. A **89**, 013815 (2014).
[20] T. Zanon, S. Guerandel, E. de Clercq, D. Holleville, N. Dimarcq, and A. Clairon, Phys. Rev. Lett. **94**, 193002 (2005).
[21] K. L. Corwin, Z. T. Lu, C. F. Hand, R. J. Epstein, and C. E. Wieman, Appl. Opt. **37**, 3295 (1998).
[22] Upon our inquiry on the excess noise of Model ZVE-3W-83+, Mini-Circuits performed a test and confirmed that the excess noise exists as we observed.